THAM 14.8

Adaptive Timing Synchronization Scheme for a Short-ranged Bluetooth Network

Young-Hwan You†, Min-Chul Ju†, Cheol-Hee Park†, Jong-Ho Paik†, and Hyoung-Kyu Song††

†System IC Research Center, Korea Electronics Technology Institute (KETI), Korea
††Department of Information & Communication Engineering, Sejong University, Korea

Abstract—**This paper describes an adaptive timing synchronization scheme of a short-ranged Bluetooth system in the partial-band noise environments. The variance of the partial-band interference is estimated and is utilized for the trigger threshold value of the inquiry scan and page scan states. Numerical results show the proposed synchronization algorithm is robust to the partial-band noise interference.**

1. Introduction

This paper is concerned with an adaptive timing synchronization scheme for the short-ranged personal area network (PAN) [1][2]. The performance of the synchronization receiver can be examined in the presence of the partial-band noise jamming in terms of the detection probability. In this paper, we consider the partial-band interference, which may be due to a partial-band jammer as well as other unwanted interferences, and is modeled as additive Gaussian noise [3][4]. Furthermore, the interference is assumed to be present in a frequency shift keying (FSK) demodulator for any reception of the dehopped signal with probability r.

2. Adaptive Timing synchronization in Bluetooth Systems

The FH/GFSK receiver with an adaptive synchronization consists of two channels; one tuned to baseband frequency f_1 corresponding to "space" and the other to frequency f_2 corresponding to "mark". After down-converting and dehopping by the frequency synthesizer, the dehopped signal is then to be processed by the square-law combining FSK receiver [3]. The detector outputs are sampled once every bit duration and the difference between the outputs of two channels is correlated with the inquiry access code (IAC) or device access code (DAC) to produce correlation output Z. The estimated noise variance is multiplied by weighting factor K to produce a synchronization threshold $\sigma_k^2 K$. If the correlation output exceeds $\sigma_k^2 K$, the Bluetooth unit will transit inquiry response state, responding a frequency hop synchronization (FHS) packet, when it is in the inquiry scan state and enter slave response substate, replying DAC, when in the page scan state [1].

In practice, the measurement of noise power cannot be accomplished perfectly. As described in [4], however, using reciprocal of the sum of the outputs of the two quadratic detectors achieves the same noise-limited improvement effect as the above mentioned receiver whose performance is based on the perfect estimation of noise power. For analysis purposes, therefore, we have assumed that the measurement of noise variance produces σ_k^2 exactly.

3. Detection Performance

The region of time/frequency uncertainty of the transmitted phase is divided into samples with one of them denoting the sync-sample (Hypothesis H_1) and the others the nonsync-samples (Hypothesis H_0). According to the transmitted signal ("space" and "mark"), the sampled detector output of each channel can be represented as

$$r_k^{(s/m)} = \begin{cases} \left(\Lambda_{\cos}^{(s/m),\,ik}\right)^2 + \left(\Lambda_{\sin}^{(s/m),\,2k}\right)^2, & \text{with energy} \\ n_{3k}^{(s/m)^2} + n_{4k}^{(s/m)^2}, & \text{without energy} \end{cases} \tag{1}$$

where $\Lambda_{\cos/\sin}^{(s/m),\,ik} = \sqrt{2P}\cos/\sin\theta_k^{(s/m)} + n_{ik}^{(s/m)}$, P is the signal power, $\{\theta_k^{(s/m)}\}$ are the uniform phase random variable, $\{n_{ik}^{(s/m)}\}$ are the independent zero-mean Gaussian with variance σ_k^2 in each channel, and (s/m) notation denotes the corresponding term-wise pair.

Under the assumption of the same average noise power in both "mark" and "space" channels, after correlating the difference between the outputs of two channels with IAC or DAC, the output of the correlator of H_1 sample is expressed as

$$Z = \frac{1}{M}\left\{\sum_{k=1}^{M_{+1}} \sigma_k^2\left[\left(\Omega_{\cos}^{(s),\,1k}\right)^2 + \left(\Omega_{\sin}^{(s),\,2k}\right)^2 - \omega_k^{(s)^2}\right] + \sum_{k=1}^{M_{-1}} \sigma_k^2\left[\left(\Omega_{\cos}^{(m),\,1k}\right)^2 + \left(\Omega_{\sin}^{(m),\,2k}\right)^2 - \omega_k^{(m)^2}\right]\right\} \tag{2}$$

where $\Omega_{\cos/\sin}^{(x),\,ik} = \sqrt{2P/\sigma_k^2}\cos/\sin\theta_k^{(x)} + w_{ik}^{(x)}$, $\omega_k^{(x)^2} = w_{3k}^{(x)^2} + w_{4k}^{(x)^2}$, $M = M_{+1} + M_{-1}$, $\{w_{ik}^{(s/m)}\}$ are independent Gaussian random variables with zero mean and unit variance, and the received noise power of

0-7803-6301-9/00 $10.00 © 2000 IEEE

each channel is $\sigma_k^2 = N_0 B$ with probability $1 - r$ and $\sigma_k^2 = (N_0 + N_J/r)B$ with probability r, respectively. M_{+1} is the number of one's in the access code, M_{-1} is the number of zero's in the access code, B is the cell bandwidth, and N_0 and N_J are the thermal noise spectral density and the average jamming noise spectral density, respectively.

To evaluate the probability distribution function (PDF) of correlation output, based on the central limit theorem, we have assumed that the correlation term is Gaussian [5]. Fortunately, since a 64-bit synchronization word is used in the Bluetooth system (i.e., $M = 64$), such an approximation is certainly feasible. From the above discussion, the PDF of Z under hypothesis H_1 follows the Gaussian distribution with mean $2P$ and variance $8(\sigma_k^2 P + \sigma_k^4)/M$.

Under the assumption that the noise power is estimated exactly, the detection probability, P_D, is the probability that the H_1 sample exceeds the threshold $\sigma_k^2 K$, which can be evaluated as

$$P_D = (1-r)Q\left(\frac{K-2\rho_1}{\zeta_1}\right) + rQ\left(\frac{K-2\rho_2}{\zeta_2}\right) \quad (3)$$

where $Q(x) = \int_x^\infty \frac{1}{\sqrt{2\pi}} e^{-\frac{t^2}{2}} dt$, $\rho_1 = E_b/N_0$, $\rho_2 = E_b/(N_0 + N_J/r)$, and $\zeta_i = \sqrt{8(\rho_i + 1)/M}$.

4. Numerical Results and Discussions

Throughout this section the parameters $M = 64$ and $B = 1$ MHz are assumed. By adopting Neyman-Pearson criterion, the value of a weighting factor K is chosen to ensure P_{FA} an acceptable rate for each value of E_b/N_0 and E_b/N_J. Though the master does not broadcast message, the correlation output of slave's unit may exceed the threshold $\sigma_k^2 K$ due to the noise interferences. Under hypothesis H_0, this happens with probability $P_{FA} = (1-r)Q(K/\zeta_1) + rQ(K/\zeta_2)$.

Fig. 1 presents the actual trigger threshold versus E_b/N_J with $r = 0.5$ and $P_{FA} = 10^{-6}$. The solid line represents the values of K for various values of E_b/N_0 and E_b/N_J. It is clear from Fig. 1 that values of the weighting factor K is insensitive to the partial-band noise interferences and an adaptive setting of the actual trigger threshold can be obtained by setting the weighting factor to a fixed value.

Performance of the synchronization receiver for various values of partial-band jamming fractions r and E_b/N_0 with $P_{FA} = 10^{-6}$ is shown in Fig. 2. As expected, for lower E_b/N_J, the detection probability of the receiver depends heavily on the partial-band jamming noise. For a partial-band jamming fraction of $r = 1$, however, the performance degradation according to the variation of E_b/N_0 is negligible, which is thanks to the deemphasis of jammed hops provided by the nonlinear combining scheme. The output of correlation detector when a hop contains a large amount of interference will be smaller than the output when interference is not present, and the hops without interference will have a greater influence on the detection performance. Especially, this scheme is suitable for the low-cost and low-complexity technologies like Bluetooth, HomeRF, and HomeCast.

References

[1] Bluetooth SIG groups, "Specification of the bluetooth system," ver 1.0 draft foundation, July 1999.

[2] HomeRF, "Technical summary of the SWAP specification," February 1999.

[3] J. S. Lee, R. H. French, and L. E. Miller, "Probability of error analyses of a BFSK frequency-hopping system with diversity under partial-band jamming interference-Part I: Performance of a square-law linear combining soft decision receiver," *IEEE Trans. Commun.*, vol. 32, no. 6, pp. 645-653, June 1984.

[4] L. E. Miller, J. S. Lee, and A. P. Kadrichu, "Probability of error analyses of a BFSK frequency-hopping system with diversity under partial-band jamming interference-Part III: Performance of a square-law self-normalizing soft decision receiver," *IEEE Trans. Commun.*, vol. 34, no. 7, pp. 669-675, July 1986.

[5] J. G. Proakis, *Digital Communications*, 2nd Ed. New York: MacGraw-Hill, 1989.

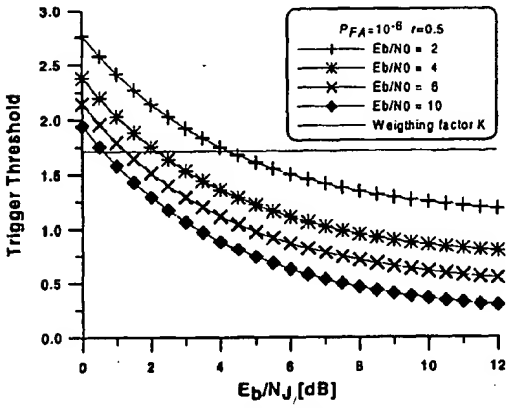

Fig. 1. Trigger threshold versus E_b/N_J for various values of E_b/N_0 with $P_{FA} = 10^{-6}$ and $r = 0.5$

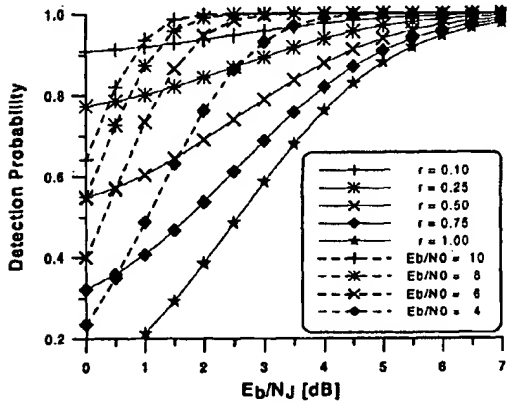

Fig. 2. Performance of the synchronization receiver for various values of r and E_b/N_0 with $P_{FA} = 10^{-6}$: (1) solid line - $E_b/N_0 = 2$ [dB] and (2) dashed line - $r = 1.0$

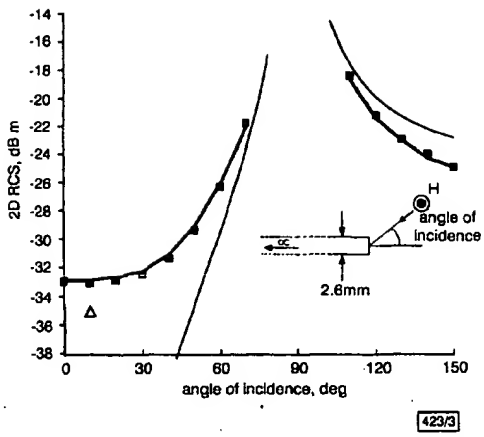

Fig. 3 *Measured and predicted 2D diffraction RCS of 2.6mm PEC halfplane edge at 10GHz*

predicted halfplane (FDTD)
measured halfplane (2D range)
zero thickness halfplane
measured halfplane (conventional range)

The diffraction RCS of a halfplane edge is shown in Fig. 3. The thickness of the edge is 2.6mm and the test frequency is 10GHz. For comparison, two further data sets are shown; the predicted 2D RCS of a diffracting edge of zero thickness (after [7]), and the 2D RCS of the 2.6mm edge as measured on a conventional radar range using a triangular LO test piece and the methodology described in [5]. The interval $70 \leq \theta \leq 110$ is omitted in Fig. 3 because of the contributions from specular reflections. For $\theta > 150$, computational limitations prevent accurate numerical prediction of the edge's RCS. Fundamental experimental limitations prevent measurement when $160 \leq \theta \leq 200°$.

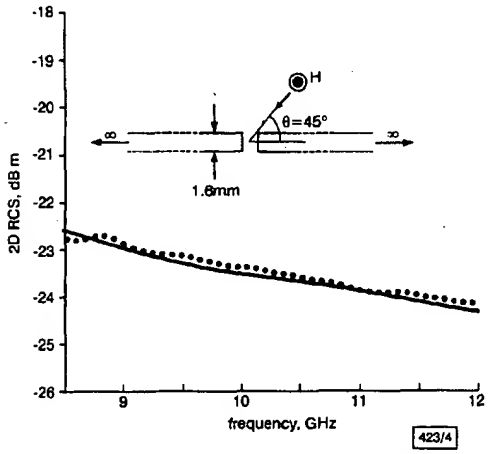

Fig. 4 *Measured and predicted 2D RCS of parallel-edged gap in otherwise conducting plane of infinite extent*

Gap width is 5mm
measured
predicted

The diffraction RCS at $\theta = 45°$ of a 2D gap in an otherwise infinite conducting plane is shown in Fig. 4. An estimate of the minimum measurable diffraction RCS at $\theta = 45°$ can be obtained by replacing the 2D gap sample with a second sample which mimics an infinite conducting plane. Measurements on the second sample at $\theta = 45°$ result in a maximum 2D RCS in the band 8.5–12.0GHz of –65dBm, due mainly to stray specular reflections from the mirror's supporting structure.

Differences between predicted and measured data are due primarily to the fundamental accuracy limitations of the experimental method; these limitations rest on the finite accuracy of the microwave receiving equipment, the finite width of the Gaussian beam and the beam's modal purity. Additional differences between predicted and measured data are caused by (i) inaccuracy in the numerical FDTD solutions (except Fig. 2 which uses an analytic solution), (ii) inaccuracy of the sample positioner, and (iii) reflections from the metal base plate which supports the mirror/horn assembly (the major source of error in the E polarised data of Figs. 2 and 4). Further reductions in the effects of (ii) and (iii) on measured data are possible.

Conclusions: A technique has been described for measuring the 2D RCS of quasi-2D structures. The results indicate that the method is subject to low uncertainties (< 0.3dBm) for a broad range of measurement parameters. The technique has applications to oblique incidence measurements with the constraint that the sample length is increased. At oblique angles the ends of the quasi-2D sample may require termination with an absorbing material to prevent the re-radiation of surface guided waves. The technique can be used to measure the diffraction coefficient of an impedance discontinuity if the calibration cylinder is replaced with a conducting wedge.

22 February 2000
Electronics Letters Online No: 20000591
DOI: 10.1049/el:20000591

F.C. Smith (*School of Engineering, University of Hull, Hull, HU6 7RX, United Kingdom*)

References

1 UFIMTSEV, P.Y.: 'Comments on diffraction principles and limitations of RCS reduction techniques', *IEEE Proc.*, 1996, **84**, (12), pp. 1830–1851
2 BURNSIDE, W.D., and BURGENER, K.W.: 'High frequency scattering by a thin lossless dielectric slab', *IEEE Trans.*, 1983, **AP-31**, (1), pp. 104–110
3 ANDERSON, H.R.: 'Building corner diffraction measurements and predictions using UTD', *IEEE Trans.*, 1998, **AP-46**, (2), pp. 292–293
4 DEMETRESCU, C., CONSTANTINOU, C.C., and MEHLER, M.J.: 'Scattering by a right-angled lossy dielectric wedge', *IEE Proc.*, 1997, **MAP-144**, (5), pp. 392–396
5 KOHIN, M.: 'Scatter measured from impedance discontinuities', *IEEE Trans.*, 1996, **AP-44**, (4), pp. 532–538
6 SMITH, F.C.: 'Investigations into non-specular scattering – Part 1, The measurement of diffraction RCS.' Final Report for DERA Contract 230Z128, University of Hull, UK, February 2000, pp. 12–21
7 BUCCI, O.M., and FRANCESCHETTI, G.: 'Electromagnetic scattering by a half-plane with two face impedances', *Radio Sci.*, 1976, **11**, (1), pp. 49–59

Adaptive timing synchronisation scheme for short-range Bluetooth network

Young-Hwan You, Min-Chul Ju, Cheol-Hee Park, Jong-Ho Paik and Hyoung-Kyu Song

An adaptive timing synchronisation scheme for a short-range Bluetooth system in partial-band noise environments is presented. The variance of the partial-band interference is estimated and is used for the trigger threshold value of the inquiry scan and page scan states. Numerical results show the proposed synchronisation algorithm is robust to partial-band noise interference and is of low complexity, which makes it suitable for use in low-cost personal area networks.

Introduction: Recently, much attention has been paid to a new class of home- and personal-area network (PAN) devices. Utilising low-cost technologies such as HomeRF, HomeCast, and Bluetooth, they will use wireless links to both access wide-area communications and exchange data among themselves [1, 2]. In particular, Bluetooth is a low-cost short-range radio link, facilitating protected *ad-hoc* connections for stationary and mobile communication environments [1].

Bluetooth transceivers operate in the unlicensed 2.4GHz ISM band. Cordless telephones, garage door openers, microwave ovens, and other PAN devices such as HomeRF and IEEE 802.11 also operate in this band and among these devices microwave ovens are the strongest source of interference. In the Bluetooth system, using a frequency-hop (FH) technique and error correction algorithms, interference protection can be achieved [1]. In the inquiry scan and page scan procedure, however, the interferences from other PAN devices operating in the ISM band will prevent Bluetooth units from establishing reliable synchronisations and connections.

In this Letter we are concerned with an adaptive timing synchronisation scheme during the inquiry scan and page scan substate of the Bluetooth system. The performance of the synchronisation receiver can be examined in the presence of partial-band noise jamming in terms of the detection probability. In this Letter, we consider partial-band interference, which may be due to the presence of a partial-band jammer as well as other unwanted interferences, and is modelled as additive Gaussian noise [3, 4]. Furthermore, the interference is assumed to be present in a frequency shift keying (FSK) demodulator for any reception of the dehopped signal with probability r.

Adaptive timing synchronisation in Bluetooth systems: The FH/GFSK receiver with adaptive synchronisation consists of two channels: one tuned to baseband frequency f_1 corresponding to a 'space' and the other to frequency f_2 corresponding to a 'mark'. After downconverting and dehopping by the frequency synthesiser, the dehopped signal is then processed by the square-law combining FSK receiver [3]. The detector outputs are sampled once every bit duration and the difference between the outputs of two channels is correlated with the inquiry access code (IAC) or device access code (DAC) to produce correlation output Z. The estimated noise variance is multiplied by weighting factor K to produce a synchronisation threshold $\sigma_k^2 K$. If the correlation output exceeds $\sigma_k^2 K$, the Bluetooth unit will move through the inquiry response state, responding to a frequency hop synchronisation (FHS) packet, when it is in the inquiry scan state and enter the slave response substate, replying DAC, when in the page scan state [1].

In practice, the measurement of noise power cannot be accomplished perfectly. As described in [4], however, use of the reciprocal of the sum of the outputs of the two quadratic detectors achieves the same noise-limited improvement effect as the above mentioned receiver, the performance of which is based on the perfect estimation of noise power. For analysis purposes, therefore, we have assumed that the measurement of noise variance produces σ_k^2 exactly and the pulse response of a Gaussian lowpass filter (LPF) is rectangular.

Detection performance: The region of time/frequency uncertainty of the transmitted phase is divided into samples with one of them denoting the sync-sample (hypothesis H_1) and the others the non-sync-samples (hypothesis H_0). According to the transmitted signal ('space' and 'mark'), the sampled detector output of each channel can be represented as

$$r_k^{(s/m)} = \begin{cases} \left(\Lambda_{\cos}^{(s/m),1k}\right)^2 + \left(\Lambda_{\sin}^{(s/m),2k}\right)^2 & \text{if energy detected} \\ n_{3k}^{(s/m)^2} + n_{4k}^{(s/m)^2} & \text{if energy not detected} \end{cases} \quad (1)$$

where $\Lambda_{\cos/\sin}^{(s/m),ik} = \sqrt{(2P)}\cos/\sin\theta_k^{(s/m)} + n_{ik}^{(s/m)}$, P is the signal power, $\{\theta_k^{(s/m)}\}$ represents the uniform phase random variables, $\{n_{ik}^{(s/m)}\}$ the independent zero-mean Gaussian with variance σ_k^2 in each channel, and (s/m) denotes the corresponding term-wise pair.

Under the assumption of the same average noise power in both 'mark' and 'space' channels, after correlating the difference between the outputs of two channels with an IAC or DAC, the output of the correlator of H_1 sample is expressed as

$$Z = \frac{1}{M}\left\{\sum_{k=1}^{M_{+1}} \sigma_k^2\left[\left(\Omega_{\cos}^{(s),1k}\right)^2 + \left(\Omega_{\sin}^{(s),2k}\right)^2 - \omega_k^{(s)^2}\right] + \sum_{k=1}^{M_{-1}} \sigma_k^2\left[\left(\Omega_{\cos}^{(m),1k}\right)^2 + \left(\Omega_{\sin}^{(m),2k}\right)^2 - \omega_k^{(m)^2}\right]\right\} \quad (2)$$

where $\Omega_{\cos/\sin}^{(x),ik} = \sqrt{(2P/\sigma_k^2)}\cos/\sin\theta_k^{(x)} + w_{ik}^{(x)}$, $w_k^{(x)^2} = w_{3k}^{(x)^2} + w_{4k}^{(x)^2}$, $M = M_{+1} + M_{-1}$, $\{w_{ik}^{(s/m)}\}$ are independent Gaussian random variables with zero mean and unit variance, and the received noise power of each channel is $\sigma_k^2 = N_0 B$ with probability $1 - r$ and $\sigma_k^2 = (N_0 + N_J/r)B$ with probability r, respectively. M_{+1} is the number of ones in the access code, M_{-1} is the number of zeros in the access code, B is the cell bandwidth, and N_0 and N_J are the thermal noise spectral density and the average jamming noise spectral density, respectively.

To evaluate the probability distribution function (PDF) of the correlation output, based on the central limit theorem, we have assumed that the correlation term is Gaussian [5]. Fortunately, since a 64 bit synchronisation word is used in the Bluetooth system (i.e. $M = 64$), such an approximation is certainly feasible. From the above discussion, the PDF of Z under hypothesis H_1 follows the Gaussian distribution with mean $2P$ and variance $8(\sigma_k^2 P + \sigma_k^4)/M$.

Under the assumption that the noise power is estimated exactly, the detection probability, P_D, is the probability that the H_1 sample exceeds the threshold $\sigma_k^2 K$, which can be evaluated as

$$P_D = (1 - r)Q\left(\frac{K - 2\rho_1}{\zeta_1}\right) + rQ\left(\frac{K - 2\rho_2}{\zeta_2}\right) \quad (3)$$

where $Q(x) = \int_x^\infty (1/\sqrt{(2\pi)})e^{-t^2/2}dt$, $\rho_1 = E_b/N_0$, $\rho_2 = E_b/(N_0 + N_J/r)$, and $\zeta_i = \sqrt{[8(\rho_i + 1)/M]}$.

Numerical results and discussions: In this Section the parameters $M = 64$ and $B = 1$MHz are assumed. By adopting the Neyman-Pearson criterion, the value of weighting factor K is chosen to ensure that P_{FA} is an acceptable rate for each value of E_b/N_0 and E_b/N_J. Although the master does not broadcast a message, the correlation output of the slave unit may exceed the threshold $\sigma_k^2 K$ due to the noise interference. Under hypothesis H_0, this happens with probability $P_{FA} = (1 - r)Q(K/\zeta_1) + rQ(K/\zeta_2)$.

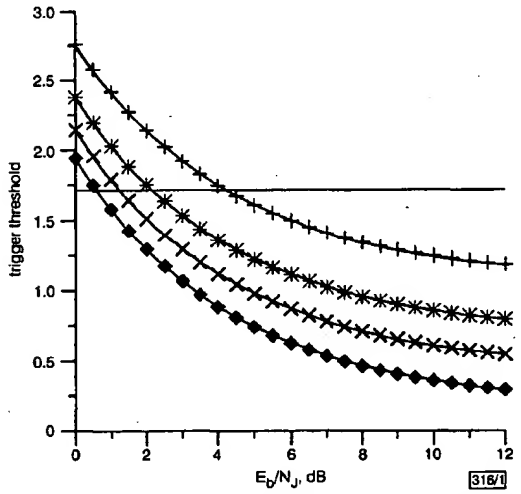

Fig. 1 *Trigger threshold against Eb/N$_J$ for various values of E_b/N_0 with $P_{FA} = 10^{-6}$ and $r = 0.5$*

—+— $E_b/N_0 = 2$
—✳— $E_b/N_0 = 4$
—×— $E_b/N_0 = 6$
—◆— $E_b/N_0 = 10$
——— weighting factor K

Fig. 1 shows the actual trigger threshold against E_b/N_J with $r = 0.5$ and $P_{FA} = 10^{-6}$. The solid line represents the values of K for various values of E_b/N_0 and E_b/N_J. It is clear from Fig. 1 that the weighting factor K is insensitive to the partial-band noise interference and an adaptive setting of the actual trigger threshold can be obtained by setting the weighting factor to a fixed value.

The performance of the synchronisation receiver for various values of partial-band jamming fractions r and E_b/N_0 with $P_{FA} = 10^{-6}$ is shown in Fig. 2. As expected, for lower E_b/N_J, the detection probability of the receiver depends heavily on the partial-

band jamming noise. For a partial-band jamming fraction of $r = 1$, however, the performance degradation according to the variation of E_b/N_0 is negligible, which is due to the de-emphasis of jammed hops provided by the nonlinear combining scheme. The output of the correlation detector when a hop contains a large amount of interference will be smaller than the output when interference is not present, and the hops without interference will have a greater influence on the detection performance.

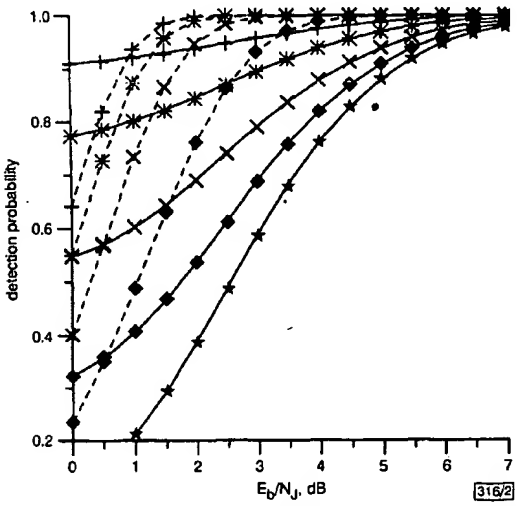

Fig. 2 *Performance of synchronisation receiver for various values of r and E_b/N_0 with $P_{FA} = 10^{-6}$*

——— Eb/N_0 = 2 dB
– – – – r = 1.0
—+— r = 0.10
—✳— r = 0.25
—×— r = 0.50
—◆— r = 0.75
—★— r = 1.00
– – + – – E_b/N_0 = 10
– – ✳ – – E_b/N_0 = 8
– – × – – E_b/N_0 = 6
– – ◆ – – E_b/N_0 = 4

Conclusions: The detection performance of the proposed synchronisation receiver for a short-range radio system has been addressed in partial-band noise environments. Its synchronisation performance is robust against partial-band noise. In particular, this scheme is suitable for low-cost and low-complexity technologies such as Bluetooth, HomeRF, and HomeCast.

16 February 2000
Electronics Letters Online No: 20000617
DOI: 10.1049/el:20000617

Young-Hwan You, Min-Chul Ju, Cheol-Hee Park and Jong-Ho Paik (*System IC Research Center, Korea Electronics Technology Institute (KETI), Korea*)

Hyoung-Kyu Song (*Department of Information & Communication Engineering, Sejong University, Korea*)

References

1 Bluetooth SIG groups: 'Specification of the bluetooth system'. Ver 1.0 Draft Foundation, July 1999

2 HomeRF: 'Technical summary of the SWAP specification'. Feb. 1999

3 LEE, J.S., FRENCH, R.H., and MILLER, L.E.: 'Probability of error analyses of a BFSK frequency-hopping system with diversity under partial-band jamming interference — Part I: Performance of a square-law linear combining soft decision receiver', *IEEE Trans.*, 1984, **COM-32**, (6), pp. 645–653

4 MILLER, L.E., LEE, J.S., and KADRICHU, A.P.: 'Probability of error analyses of a BFSK frequency-hopping system with diversity under partial-band jamming interference — Part III: Performance of a square-law self-normalizing soft decision receiver', *IEEE Trans.*, 1986, **COM-34**, (7), pp. 669–675

5 PROAKIS, J.G.: 'Digital communications' (MacGraw-Hill, New York, 2nd Edn., 1989)

Analysis of intermodulation distortion in log-normal shadowed WLAN channels

M. Wennström, T. Öberg and A. Rydberg

In wireless local area network systems using multicarrier modulation, intermodulation distortion (IMD) occurs due to the nonlinear transmission amplifier and the non-constant envelope of the transmitted signals. A closed form expression is presented for the blocking probability assuming a log-normal distributed fading channel. The result is verified using Monte Carlo simulations.

Introduction: Multicarrier modulation techniques such as orthogonal frequency division multiplexing (OFDM) are often proposed for use in wireless local area networks (WLANs) to mitigate the multipath and time dispersive channels of high-bit-rate indoor systems. The multicarrier technique is effective since each subcarrier is modulated with a low bit rate, thus resulting in a symbol period much longer than typical echo delays. Any multicarrier signal has a large peak-to-mean envelope power ratio and, when passed through a nonlinear device such as a transmitter power amplifier, intermodulation distortion (IMD) is generated. Owing to the near-far ratio of two users connected to a WLAN access point (AP), the IMD generated by a near transmitter might block a far transmitter. This blocking will manifest itself as a reduction in the system capacity from that of the ideal case.

Often, in a WLAN environment, shadow fading is caused due to obstacles such as office furniture and walls, which leads to signal fading on a large scale. It is often modelled as a log-normal distribution around the mean given by a path loss equation.

The question to be answered in this Letter is what level of IMD can be tolerated for a given allowed probability of blocking. The problem was earlier addressed in [1] where a closed form expression was derived that characterises the relationship between the blocking probability and linearity requirements of the power amplifier in a simple channel with an inverse power law attenuation of the signal power. In this Letter, we present the corresponding closed form expression for the blocking probability in the log-normal fading case. The presented results have been verified by Monte Carlo simulations.

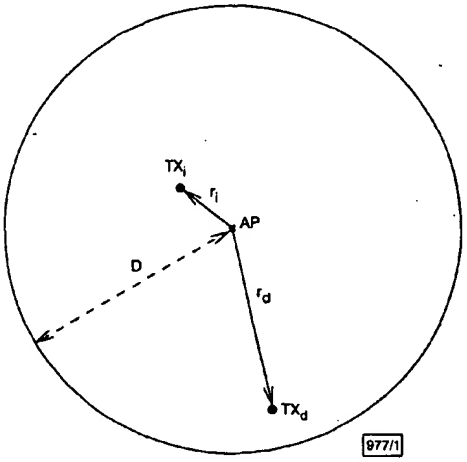

Fig. 1 *Near far scenario where IMD from TX_i is interfering with signal from TX_d at AP*

D is maximum range of AP

Analysis: Our assumptions are similar to the assumptions in [1] where an AP is the receiver (RX), and the desired transmitter TX_d and an interfering transmitter TX_i are situated at a distance r_d and r_i from the AP, respectively, see Fig. 1. The maximum range for the AP coverage is D. In the analysis of this problem we make some assumptions to obtain an analytically tractable problem. We assume that the transmitters are transmitting with the same power and without power control. The transmitter positions are independent and uniformly area distributed over a disc of radius D from the AP. When the desired signal power to IMD power ratio